CHAPTER V

NOVEL CARBONIZED, GOLD/GRAPHENE HYBRID NANOWIRE-MODIFIED DISPOSABLE ELECTRODE FOR THE ULTRASENSITIVE AND SELECTIVE DETECTION OF DOPAMINE IN BIOLOGICAL SAMPLES

5.1 Abstract

A new type of biosensor was fabricated using a carbonized hybrid gold (Au)/graphene (G) nanowire constructed on a disposable screen-printed carbon electrode (SPCE) for signal amplification. Electrospinning and carbonization processes were combined to achieve the selective and sensitive determination of dopamine (DA) in the presence of ascorbic acid (AA) and uric acid (UA). Scanning electron microscopy, transmission electron microscopy and X-ray diffraction were used to characterize the surface morphology and physical properties of the products before and after carbonization. The electrochemical behavior of the modified electrode (CPAN-Au/G) in $[Fe(CN)_6]^{3-/4-}$ and DA was studied by cyclic voltammetry (CV) and differential pulse voltammetry (DPV). The results confirmed that the modified electrode was effective for the selective detection of dopamine (DA) in the presence of interfering substances in 0.1 M PBS at pH 7.4 without using an anionic surfactant as the discriminating agent. The DPV current showed a linear dependence on DA concentrations ranging from 0.001 to 60 μM with a limit of detection of 0.8 nM (S/N=3) and a sensitivity of 1.4351 μAcm^{-2}. The CPAN-Au/G electrode successfully determined the DA levels in human serum. The modified electrode could be a promising candidate for use as a high-potential electrode, representing a new approach for the selective and sensitive determination of dopamine with long-term sensor stability.

Keywords: Dopamine, Carbonization, Graphene, Electrospun Nanofiber, Carbon Screen-printed Electrode, Gold nanoparticle, Nanowire

5.2 Introduction

Dopamine (DA) plays an important role in the physiological function of organisms. Abnormal levels of DA have been correlated with Parkinson's disease (Sauerbier, 2013, Zhang, 2007), Alzheimer's disease (Liu, 2011), and schizophrenia (Heinz, 1995) and can alter the relationship between neuron behavior and psychology (Venton, 2003). Numerous analytical techniques have been used to detect DA, including chromatography (Song, 2012), capillary electrophoresis (Wallenborg, 1999), spectrofluorometry (Huang, 2012), and surface plasmon resonance (Kumbhat, 2007). These techniques are time consuming and complicated, and they require specialized laboratory equipment (Rattanarat, 2012). Therefore, electrochemical analyses have attracted interest because of their high sensitivity, low cost, rapid detection rate, and effectiveness in diverse biological environments (Wightman, 2006). The presence of interfering substances poses the principal challenge to the electrochemical detection of DA in complex biological samples. Substances such as ascorbic acid (AA) and uric acid (UA) oxidize at potentials similar to DA and are typically present at higher concentrations. In an organism, DA, AA, and UA usually coexist in the extracellular fluid of the central nervous system and serum. These biomolecules are very difficult to distinguish using traditional electrodes, such as bare screen-printed carbon electrodes (SPCE) and glassy carbon electrodes (GCE), because of overlapping oxidation peaks. However, recent reports have demonstrated that anionic surfactants such as sodium dodecyl sulfate (SDS) (Rattanarat, 2012, Zheng *et al.*, 2008) and cetyltrimethyl ammonium bromide (CTAB) (Hosseinzadeh *et al.*, 2009, Yang *et al.*) can be used to selectively determine DA in the presence of interfering substances. Conversely, other studies have found that using large amounts of surfactants in the measuring system could significantly disturb the oxidation current of DA (Rattanarat, 2012). Therefore, the determination of DA without using a surfactant or altering the pH is desirable and convenient for DA detection in biological samples.

Graphene (G) nanoparticles are a flat monolayer of carbon atoms tightly packed into a two-dimensional (2D) honeycomb lattice. They have been widely used in the fabrication of electrochemical biosensors with excellent electrical conductivity

(Alwarappan, 2009, Li, 2012) and mechanical strength (Nataraj, 2012), a large surface-to-volume ratio, and appropriate chemical stability (Zhu, 2013). G extraordinary properties establish the potential for applications to determine a variety of electro-active species, including dopamine (Kim, 2010, Liu, 2012), ractopamine (Bai, 2014), hydrogen peroxide (Gao, 2013, Ruan, 2013), and metal ions (Zhang, 2013). In addition, G can be integrated into more complex assemblies to form other advanced composites with materials such as gold (Au) (Niu *et al.*, 2013, Zhang, 2013), silver (Ag) (Huang, 2014, Zhong, 2013), and platinum (Pt) (Araque, 2014, Eremia, 2013), increasing its versatility as an advanced electrode material for high performance biosensors (Huang, 2014). Gold nanoparticles have several advantages, including faster electron transfer ability, higher surface area, and the ability to link various biofunctional groups using diverse chemical reactions (Luo, 2013, Wang, 2013). Carbonized composite nanofibers are also interesting for the fabrication of electrodes because of their wide variety of applications and straightforward production through electrospinning. After stabilization and carbonization, carbonized nanofibers form a ladder structure *via* nitrile polymerization (Nataraj, 2012), and this structure exhibits excellent conductivity and electrochemical activity (Patil, 2013). Therefore, Au/G hybrid nanowire inspired this study, and the composite could successfully enable the development of more complicated electrochemical activity for biosensing materials.

Many modified electrodes have been studied for the sensitive and selective determination of DA, including a graphene oxide (GO) / multiwall carbon nanotube (CNT) electrode (Yuan *et al.*, 2014), a GCE modified with poly(orotic acid) (Zhang *et al.*, 2013), a polystyrene-grafted graphene electrode (Liu *et al.*, 2013), and a microchip electrode with carbon nanotube (CNT) ink (Zhao, 2013). However, these electrodes are all relatively expensive and complicated to construct. To lower costs and simplify construction, several researchers have reported alternative approaches to sensing based on surface modification of disposable SPCEs (Alarcón-Ángeles, 2010, Ku, 2013, Ping, 2010, Rattanarat, 2012).

In this study, we described a dopamine biosensor based on carbonized hybrid Au/G nanowire (CPAN-Au/G) which was fabricated by a combination of electrospinning and carbonization processes. Characterization of the basic materials

and electrochemical behavior of the carbonized products were systematically studied. The CPAN-Au/G modifications were constructed on a SPCE surface. CPAN-Au/G showed an excellent differential pulse voltammetry (DPV) response to DA in the presence of typical interfering molecules (AA and UA) in 0.1 M phosphate-buffered saline (PBS) at pH 7.4 and in human serum without a discriminating agent. The results show great promise for the fabrication of a practical DA biosensor.

5.3 Experimental

5.3.1 Materials

All materials used in this study were analytical grade. G nanopowder (99.2% C) had an average flake thickness of 12 nm and was purchased from Graphene Supermarket, USA. N, N-Dimethylformamide (DMF), dopamine hydrochloride (DA), sodium dodecyl sulfate (SDS), hydrochloric acid (HCl), gold (III) chloride hydrate ($HAuCl_4 3H_2O$), sodium borohydride ($NaBH_4$), potassium ferricyanide ($K_3[Fe(CN)_6]$), potassium ferrocyanide ($K_4[Fe(CN)_6]$), AA, UA, trichloroacetic acid (TCA), 2-butoxyethyl acetate (99%), human serum, and polyphosphate-buffered saline (PBS) were purchased from Sigma-Aldrich. The polyacrylonitrile (PAN) had a molecular weight of approximately 55.5 kDa and was used as the raw material in the electrospinning process; it was obtained from Thai Acrylic Fiber (Thailand). The pH of the PBS was adjusted using 1.0 M HCl and 1.0 M NaOH. The carbon ink (C2070424D2) was purchased from the Gwent Group (Torfaen, UK). The silver chloride ink (Electrodag 7019) was obtained from Acheson Colloids. All chemicals were used as received without further purification. The electrospinning apparatus was a Gamma High Voltage Research Model D-ES30PN/M692 equipped with a DC power source.

The electrochemical measurements were performed using a potentiostat (PGSTAT302N, Metrohm, USA) at room temperature (25±1°C). Cyclic voltammetry (CV) and DPV were performed using a three-electrode system, which consisted of the modified or unmodified SPCE as the working electrode (WE), with a working area of 0.50 cm^2, an Ag/AgCl electrode as the reference electrode (RE), and a carbon plate as the counter electrode (CE).

5.3.2 Screen-printed Carbon Electrode Fabrication

The SPCEs were produced on a substrate of 10 x 25 mm^2 PVC sheets. First, silver ink was spread over the PVC surface twice using a manual screen-printing technique; the PVC was kept in a drying oven at 60°C for 60 min to evaporate any excess solvent. Second, two carbon layers were coated on the silver layer. Finally, the plastic insulator layer was coated on the top layer. All fabricated SPCEs were stored in a desiccator prior to subsequent surface modification steps.

5.3.3 Preparation of Carbonized Au/G Hybrid Nanowire

The 11 wt% PAN solution used for electrospinning was prepared by adding PAN to DMF in a glass vial followed by vigorous magnetic stirring at 60°C for 6 h. The SDS surfactant was added to obtain a 10 mM concentration and stirred until completely dissolved. Subsequently, 5% (w/w) G and 10% (w/w) $HAuCl_4 3H_2O$ powder was added to obtain the final concentrations; after the addition of the two compounds, the solutions were sonicated for 4 h with a homogenizer.

The electrospinning apparatus used to produce the nanofibers is shown in **Fig. 5.1.** A 20 ml syringe with a capillary tip (D=0.5 mm) was placed and clamped near an anode connected to a high-voltage power supply. The cathode was connected to a piece of aluminum foil, which was subjected to an applied voltage of 15 kV relative to the anode. The distance between the electrode and nozzle was 15 cm. The collected samples were labeled to indicate the presence or absence of Au and the percentage of G loaded. After electrospinning under ambient conditions, the samples containing Au were reduced using 10% (w/w) $NaBH_4$ for 5 h to ensure completion of the reduction reaction and washed 3 times with ultra-pure water (Kim *et al.*, 2008). Finally, the electrospun samples were stabilized in a muffle oven in air at 280°C for 2 h and carbonized under nitrogen at a ramp rate of 5°C min^{-1} up to 800°C, where they were held for 3 h. The carbonized nanofibers were ground to a powder and labeled with the starting letter C; for example, CPAN-G, CPAN-Au, and CPAN-Au/G represent carbonized nanofibers containing G, Au and Au/G, respectively.

5.3.4 Preparation of Modified Electrodes

Fig. 5.1 shows a schematic of the electrode fabrication process. SPCEs modified with carbonized substances and suspended in 2-butoxyethyl acetate were prepared by casting 0.8 μl of the 30 mg ml^{-1} carbonized substance on the carbon layer of the working electrodes. After drying in an oven at 60°C for 2 h, the modified electrodes were rinsed with ultra-pure water. All modified electrodes were stored in a desiccator at room temperature prior to use (Tong, 2013).

5.3.5 Physical Properties of Carbonized Nanofibers

The surface morphologies of the samples before and after carbonization were observed using a Hitachi S-4800 field-emission scanning electron microscope (SEM) and a JEOL JEM-2010 transmission electron microscope (TEM) operated at 15 kV. The SemAphore 4.0 Software was used for image processing. The X-ray data were collected using an X-ray diffractometer (Rigaku Smartlab, Japan) based on Cu-Kα radiation. The samples were scanned over a 2θ angle from 5° to 90°.

5.3.6 Cyclic Voltammetry (CV) of Modified Electrodes

The electrochemical responses of both the modified and unmodified electrodes were characterized using single-loop CV experiments, which consisted of a forward sweep in the anodic direction from –1 V vs. Ag/AgCl up to 1 V, followed by a sweep back down to –1 V. The voltammograms were measured for 0.1 M PBS at pH 7.4 at a number of scan rates to establish the background currents. To evaluate the electrochemistry, the current response of 1 mM $[Fe(CN)_6]^{3-/4-}$ and 40 μM DA in 0.1 M PBS at pH 7.4 was evaluated at a number of scan rates and corrected by subtracting the corresponding background currents. The redox activity was quantified by measuring the anodic and cathodic peak currents (i_{pa} and i_{pc}, respectively) and peak voltages (E_{pa} and E_{pc}) as functions of the root scan rate. The peak currents were measured relative to the extrapolated baseline currents according to the graphical procedure illustrated in the supplementary material. The sample volume was 50 μl for all electrochemical measurements.

5.3.7 Electrochemical Impedance Spectroscopy

Electrochemical impedance spectroscopy (EIS) was conducted using an Autolab potentiostat PGSTAT302N (Metrohm, USA). The impedance spectra for the electrodes were measured in 1 mM $[Fe(CN)_6]^{3-/4-}$ in 0.1 M PBS at pH 7.4. The frequency range of the EIS measurement was 0.01-100 kHz, and 100 data points were collected using a 10 mV signal amplitude at a bias potential of +0.4 V vs. Ag/AgCl. All experiments were performed in triplicate.

5.3.8 Differential Pulse Voltammetry (DPV) of the Modified Electrodes to Detect DA

The optimum parameters for the DPV measurements were determined in preliminary studies (data not shown) to be as follows: pulse amplitude of 150 mV, step potential of 5 mV, and a pulse period of 200 ms for scanning the potential between –0.3 and 1.6 V vs. Ag/AgCl. This optimized potential control scheme was used in further studies with 0.1 M PBS at pH 7.4.

5.3.9 Analysis of Human Serum

Human serum is a complex biological system that contains no DA. To determine the amount of DA in human serum, known DA concentrations were added to serum using the standard addition method (Rattanarat, 2012). The protein in the serum was precipitated by the TCA precipitation method (Shahrokhian, 2007), and the samples were centrifuged at 15,000 rpm for 10 min. The serum supernatant samples were retained for further study.

5.4 Results and Discussion

5.4.1 Preparation and Characterization of Carbonized Au/G Hybrid Nanowire

The Au/G hybrid nanowires were prepared from the solution of G/$HAuCl_4$/PAN by electrospinning according to previously described methods (Kampalanonwat, 2010). A schematic of the electrode construction is shown in **Fig. 5.1**. The G content in the nanofibers was approximately 5 wt% based on calculating

the net weights of G, $HAuCl_4$ and PAN in the precursor. To disperse the G particles in the PAN solution, 10 mM of the anionic surfactant SDS was used. After the electrospinning process, gold nanoparticles (AuNP) were synthesized using 10% (w/v) $NaBH_4$, which was used to reduce the Au^{3+} ions covering the nanofiber surface to the AuNP (Bai, 2014). Thus, the samples were stabilized and carbonized. The morphology and structure of the samples before and after carbonization were characterized by SEM, as illustrated in **Fig. 5.2(a)** and **5.2(b),** respectively. The G particles of the PAN-Au/G nanofibers were randomly distributed in a 3D nanofibrous web structure with a relatively uniform average diameter of 217±30 nm. Following the stabilization and carbonization steps at high temperatures (280-800°C), the composite nanofibers were heated to form a ladder structure through exothermic reactions, which may have included dehydrogenation, cyclization, and crosslinking (Karacan, 2012, Nataraj, 2012, Saha, 2012). Therefore, the diameters of the CPAN-Au/G nanofibers were slightly decreased (142±26 nm); in addition, the fibers were shortened and exhibited lower aspect ratios after grinding (Tong, 2013), as shown in **Fig. 5.2(b).** Furthermore, the TEM image in **Fig. 5.2(c)** confirmed the presence of dispersed G particle contour fibers; energy-dispersive X-ray spectroscopy (EDX) also confirmed the existence of Au in the CPAN-Au/G, as shown in **Fig. 5.2(d).**

Fig. 5.3 shows the X-ray diffraction patterns of G, PAN, PAN-G, PAN-Au/G, and CPAN-Au/G. A diffraction peak typical of G was observed at approximately $2\theta=26°$, indicating a (002) plane (Liu, 2012) and thus a hexagonal G structure (Huang, 2012). Comparing the PAN-G and PAN-Au/G results, a typical peak from the PAN-G nanofibers could be observed at $2\theta=17°$ (Gu, 2008, Molnár, 2012), and the characteristic peaks at $2\theta=38^{o}$, 44.3^{o}, 64.5^{o} and 84.6^{o} corresponded to the (111), (200), (220) and (222) crystal planes, respectively, of face-centered cubic AuNPs covering the nanofiber surface (Ahmadalinezhad *et al.*, 2011, Choma *et al.*, 2012, Tong, 2013). Following the carbonization process, the sharpness of the G peak decreased, and a small peak for (002) diffraction appeared at $2\theta=22\text{-}23°$, indicating the formation of aromatic structures through cyclization (Chae Wook Cho, 2007). Moreover, the carbonization process in this experiment exhibited an increase in the conformation of the Au layer, which was also found in previous studies involving carbonized Au/gelatin film (Kuge *et al.*, 2010).

5.4.2 Electrochemical Behavior of Modified Electrodes

The electrochemical behavior of modified/unmodified electrodes was investigated by CV in 1 mM $[Fe(CN)_6]^{3-/4-}$ as the redox couple (Njagi, 2007) (**Fig. 5.4(a)**). **Table 5.1** shows the calculated anodic current (I_{pa}), oxidation potential (E_{pa}), I_{pa}/I_{pc}, and peak potential separation ($\Delta E_p = E_{pa} - E_{pc}$) from the CV profiles. The bare SPCE showed sluggish electron transfer kinetics for the redox reaction of $[Fe(CN)_6]^{3-/4-}$ with a low anodic current density (17.7±0.2 μA cm^{-2}) and large peak separation (ΔE_p = 780 mV); the results could be related to the $[Fe(CN)_6]^{3-/4}$ redox reaction on an unmodified electrode and fouling of the bare SPCE surface by $[Fe(CN)_6]^{3-/4}$ and its oxidation products (Huang *et al.*, 2008). In contrast, the CPAN-G, CPAN-Au, and CPAN-Au/G electrodes exhibited high current density, low ΔE_p, and I_{pa}/I_{pc}~1. The smaller ΔE_p and I_{pa}/I_{pc}~1 values revealed the faster electron-transfer kinetics and excellent electrochemical sensitivity of this electrode surface (Ku, 2013). CPAN-Au/G showed the highest current density (37.7±0.6 μA cm^{-2}) of the modified electrodes. Therefore, CPAN-Au/G was chosen for further electrochemical studies.

Fig. 5.5 illustrates the characteristic CV data of CPAN-Au/G and bare SPCE electrodes in 0.1 M PBS at pH 7.4 at various scan rates (20-400 mVs^{-1}). Upon increasing the scan rate, the anodic and cathodic current increased linearly, and the oxidation peak and reduction peak potentials shifted slightly (Ku, 2013). The oxidation peak current, I_{pa}, and reduction peak current, I_{pc}, were assumed to follow the Randle-Sevick relation,

$$I_p = kn^{3/2}AD^{1/2}C^b\upsilon^{1/2} \quad (1)$$

where the constant k is equal to 2.72×10^5; n is the number of moles of electrons transferred per mole of electroactive species ($[Fe(CN)_6]^{3-/4-}$); A is the electrode area in cm^2; D is the diffusion coefficient in $cm^2\ s^{-1}$; C^b is the bulk solution concentration in mol L^{-1}; and υ is the potential scan rate in Vs^{-1}. Generally, the peak current I_p is linearly proportional to the bulk concentration of the electroactive species, C^b, and to the square root of the scan rate, $\upsilon^{1/2}$. The anodic and cathodic peaks exhibited nearly equal peak currents. A linear relationship was observed between the peak current and the square root of the scan rate; the inset in Fig. 4(b) shows the relationship of $[Fe(CN)_6]^{3-/4-}$ at the CPAN-Au/G electrode. The increase in peak spread suggested a

quasi-reversible electrode reaction. Moreover, the incorporation of Au/G nanoparticles in the carbonized nanowire on the SPCE surface made the CPAN-Au/G system quasi-reversible (I_{pa}/I_{pc} ~1).

EIS is a powerful, nondestructive, and informative technique that has played an essential role in the kinetic characterization of events occurring at different types of electrode/solution interfaces in a wide range of applied DC (Shervedani *et al.*, 2011). Nyquist plots of the impedance spectra show semicircular and linear regions. The semicircular region provides information about interfacial charge-transfer resistance (R_p), whereas the low-frequency Warburg region signifies a diffusion process (Liu, 2012). The R_p can be used to explain the interfacial properties of the electrode (Atta, 2012), and the recorded R_p of each electrode is shown in **Fig. 5.4(c)** and **Table 5.1**. The CPAN-Au/G electrode exhibited the smallest semicircular region (R_p=11 kΩ) compared to bare SPCE (R_p=56 kΩ), CPAN-G (R_p=43 kΩ), and CPAN-Au (R_p=18 kΩ), suggesting that a low charge-transfer resistance promoted electro-oxidation and enhanced the catalytic activity of the modified electrode (Atta, 2012, Ekabutr, 2013). In addition, previous reports have shown the existence of G particles on the electrode surface which promotes the electron transfer rate of $[Fe(CN)_6]^{3-/4-}$ and enhances the sensitivity of sensors (Kim, 2010, Liu, 2012).

5.4.3 Determination of DA at Different Modified Electrodes

The differential pulse voltammograms (DPVs) of DA using various electrodes are shown in **Fig. 5.4(d),** and the collected anodic current density and oxidation potential values are shown in **Table 5.1**. In this study, each electrode was evaluated in PBS solution at pH 7.4. The CPAN-Au/G exhibited the highest anodic current density (8.16±0.1 μAcm^{-2}) with the lowest oxidation potential (-0.03 V) compared to the bare SPCE and other modified electrodes. The higher anodic current and negatively shifted oxidation potential demonstrated that the CPAN-Au/G electrode could effectively enhance the oxidation of DA. Both the CV of $[Fe(CN)_6]^{3-/4-}$ and the DPV of DA experiments demonstrated that the Au/G hybrid composite possessed good electrocatalytic activity toward the oxidation of these molecules. The three-dimensional gold nanowire provided a higher surface area to induce faster

electron transport, which may have contributed to the high electrocatalytic activity of these composites (Hsu *et al.*, 2012).

5.4.4 Effect of Solution pH

The solution pH is a vital factor in the electrochemical reaction of DA. The effect of changing the pH of the supporting electrolyte on the electrochemical behavior of DA was studied. **Fig. 5.5** shows the DPV profiles of 40 μM DA in 0.1 M PBS at pH 2.00, 4.00, 6.00, 7.40, and 8.00 on the CPAN-Au/G electrode. **Fig. 5.8** shows that the solution pH of the supporting electrolyte altered both the anodic current peak and the potential peak of DA. A large anodic peak current was obtained in the range of pH 2-7.4. In addition, the peak potential shifted negatively as the pH of the solution increased. The anodic peak potential (E_{pa}) was proportional to the solution pH in the range of 2-7.4, and it fit the linear regression equation (Eq. (2)) with a correlation coefficient of R^2= 0.9952.

$$E_{pa}=(0.327) - (0.0519)pH \quad (2)$$

These results indicated that the charge transfer process was preceded by protonation with the same number of protons involved in the DA oxidation mechanism on the CPAN-Au/G electrode surface (Atta, 2012, Bai, 2014). Conversely, **Fig. 5.8** shows that the acidity of the PBS solution also had a slight effect on the anodic current. Thus, the original PBS solution at pH 7.4 was preferred without adjustment of acidity for all DA determination experiments.

5.4.5 Analysis of Ternary Mixtures of DA, UA, and AA at the CPAN-Au/G Electrode

Figs. 5.6(a) and **5.6(b)** show typical DPV trace profiles for the individual determination of DA, UA, AA, and mixtures of these compounds at bare SPCE and CPAN-Au/G electrodes, respectively, in 0.1 M PBS at pH 7.4 (simulated human bodily fluid). AA and UA are typically found in human bodily fluids at concentrations 100- to 1,000-fold higher than DA (Atta, 2011, Rattanarat, 2012). In human serum, the typical levels of AA and UA are 80 and 400 μM, respectively (Chauhan, 2011); in this study, the concentrations of AA and UA in the supporting electrolyte were maintained at those concentrations. The anodic current and oxidation potential of DA, AA, and UA with the bare SPCE appeared at 1.82±0.1 μAcm^{-2}, +200

mV; 5.92±0.4 μAcm^{-2}, +600 mV; and 10.20±0.2 μAcm^{-2}, +400 mV, respectively. The unmodified SPCE in this study and glassy carbon electrodes from previous studies were unable to distinguish mixtures of these compounds due to overlapping anodic currents (Rodthongkum, 2013). Conversely, the CPAN-Au/G electrode was able to distinguish the DA peak (-30 mV) from the UA peak (+300 mV) at high current density (8.16±0.1 μAcm^{-2} and 22.2±0.8 μAcm^{-2}, respectively). The two well-defined oxidation peaks with larger peak separations (E_{UA}-E_{DA}) of approximately 330 mV corresponded to the oxidation of DA and UA, respectively. In comparison, the current density of CPAN-Au/G was larger than the current density of bare SPCE because the Au/G hybrid nanowire could facilitate the electron transfer and increase the electrochemically active surface area of the working electrode. Interestingly, AA did not exhibit an obvious oxidation peak in this system. Previous studies reported that electrodes modified by G, which contains a high density of negative charges, also exhibit interference from AA (Hou, 2010). It was clear that DA could be selectively determined using a CPAN-Au/G electrode without interference from AA or UA. In addition, many published studies have used various anionic surfactants, such as sodium dodecyl sulfate (SDS) (Rattanarat, 2012, Zheng, 2008) and cetyltrimethyl ammonium bromide (CTAB) (Hosseinzadeh, 2009, Yang), in the acidic solution. The negatively charged anionic surfactants align on the electrode surface and allow positively charged DA^+ to easily accumulate and oxidize at the electrode surface through electrostatic interactions; these interactions allowed the peaks of DA, UA and AA to be distinguished. However, non-surfactant systems at normal pH conditions (pH=7.4) have been more interesting than surfactant systems until now.

The linear range and detection limit of DA were determined by DPV in 0.1 M PBS at pH 7.4, as shown in **Fig. 5.7(a).** The linear relationship between the DA concentration and the oxidation current was described by the equation I_{DA} $=0.0721C_{DA}+0.0010$ with a correlation coefficient of 0.9931 (n=3) in the range of 0.001-60 μM. The LOD and sensitivity were 0.8 nM (S/N=3) and 0.1435 $\mu A\ \mu M^{-1}\ cm^{-2}$, respectively. **Table 5.2** shows the LOD, LDR, and sensitivity of various modified electrodes in previous studies compared to the CPAN-Au/G electrode. CPAN-Au/G exhibited the lowest LOD with the widest range for DA detection.

5.4.6 Determination of DA in Human Serum

To verify the application of the CPAN-Au/G electrode for practical use as a DA detector in complex biological media, the same measurements were performed in human serum. Known concentrations of DA (0.5, 1, and 10 μM) were dissolved in serum, and the protein in the serum was precipitated by TCA and centrifugation. The serum supernatants were used for further DPV analysis. Recovery experiments were performed using the standard addition method by spiking 0.5, 1, and 10 μM into the serum samples. The recovery of DA ranged from 108.4% to 109.3%, and the RSD (n=3) was below 3.0%. The results suggested that the CPAN-Au/G electrode was reliable and sensitive for the detection of DA in biological samples.

5.4.7 Fouling and Stability of the Modified Electrode

Previous reports show that the adsorption of reaction products on bare SPCE diminished the DA oxidation performance (Lane *et al.*, 1990). To assess whether the CPAN-Au/G electrode in this study might suffer the same fouling effect over three weeks, the CPAN-Au/G was successively measured 5 times in 40 μM DA and 0.1 M PBS at pH 7.4. The DPV profiles and calculated anodic current responses are shown in Fig. 10 (supplementary data). The CPAN-Au/G electrode was only washed with milli-Q water before the subsequent measurement after keeping the electrode in desiccator for 3 weeks. After 3 weeks, the current response of 40 μM DA decreased by less than 5% of the initial response, suggesting that the CPAN-Au/G electrode had good reproducibility and stability for electrochemical applications.

5.5 Conclusions

The fabrication of a Au/G hybrid nanowire was successfully achieved by a combination of electrospinning and carbonization processes. The nanowire was embedded on the SPCE surface, which was used as the DA sensing platform. The CV and DPV results showed that CPAN-Au/G had enhanced electrochemical activity toward the ferri/ferrocyanide redox couple and DA. The CPAN-Au/G electrode was used to determine DA in the presence of AA and UA, and the results showed well-

defined oxidation peaks with larger peak separation and larger current density than other modified electrodes and bare SPCE. Although many previous studies have been reported on graphene and gold-modified electrode composites, the approach in this study was more practical, and the SPCE electrode was easy to prepare by drop casting without sacrificing high selectivity and high sensitivity. This study demonstrated that the CPAN-Au/G electrode could be promising for the construction of bioelectronics and biosensors for use in many real applications.

Acknowledgements

This work was supported in part by (1) the Chulalongkorn University Dutsadi Phiphat Scholarship, and (2) Prof. Orawan Chailapakul, Electrochemistry and Optical Spectroscopy research unit, Faculty of Science, Chulalongkorn University, Thailand. We are thankful to Prof. Schwank's research group, University of Michigan, USA for the use of their muffle oven.

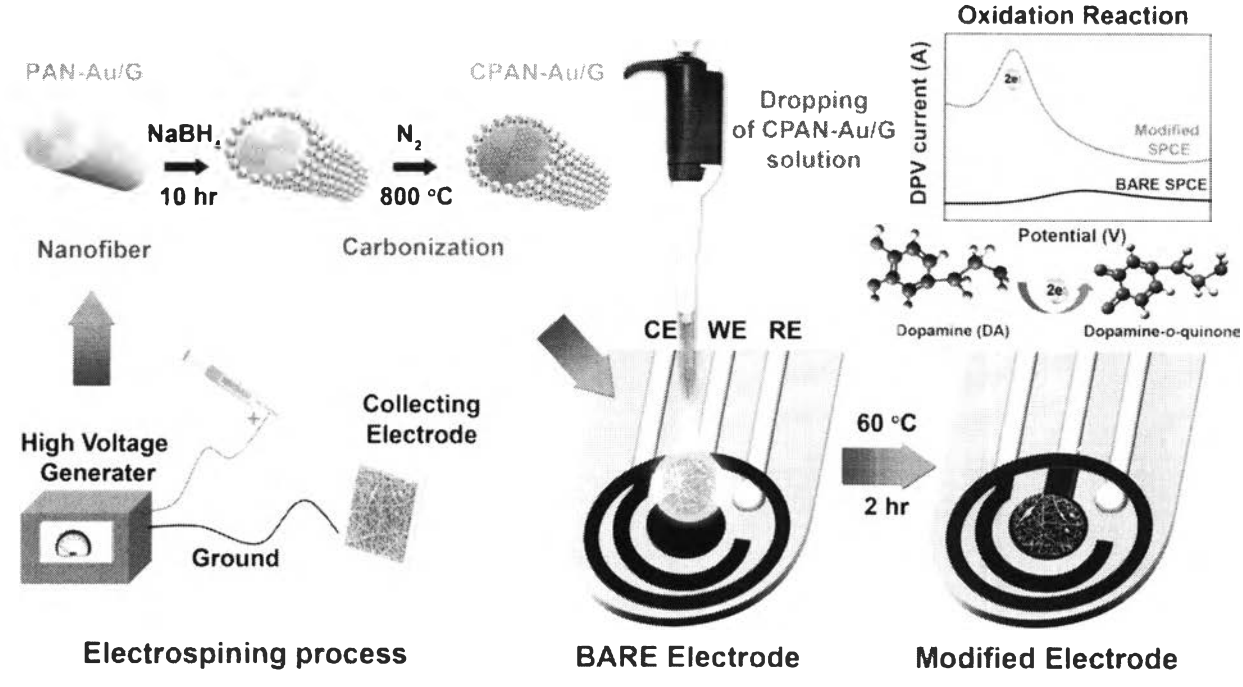

Figure 5.1 Schematic of SPCE surface modification.

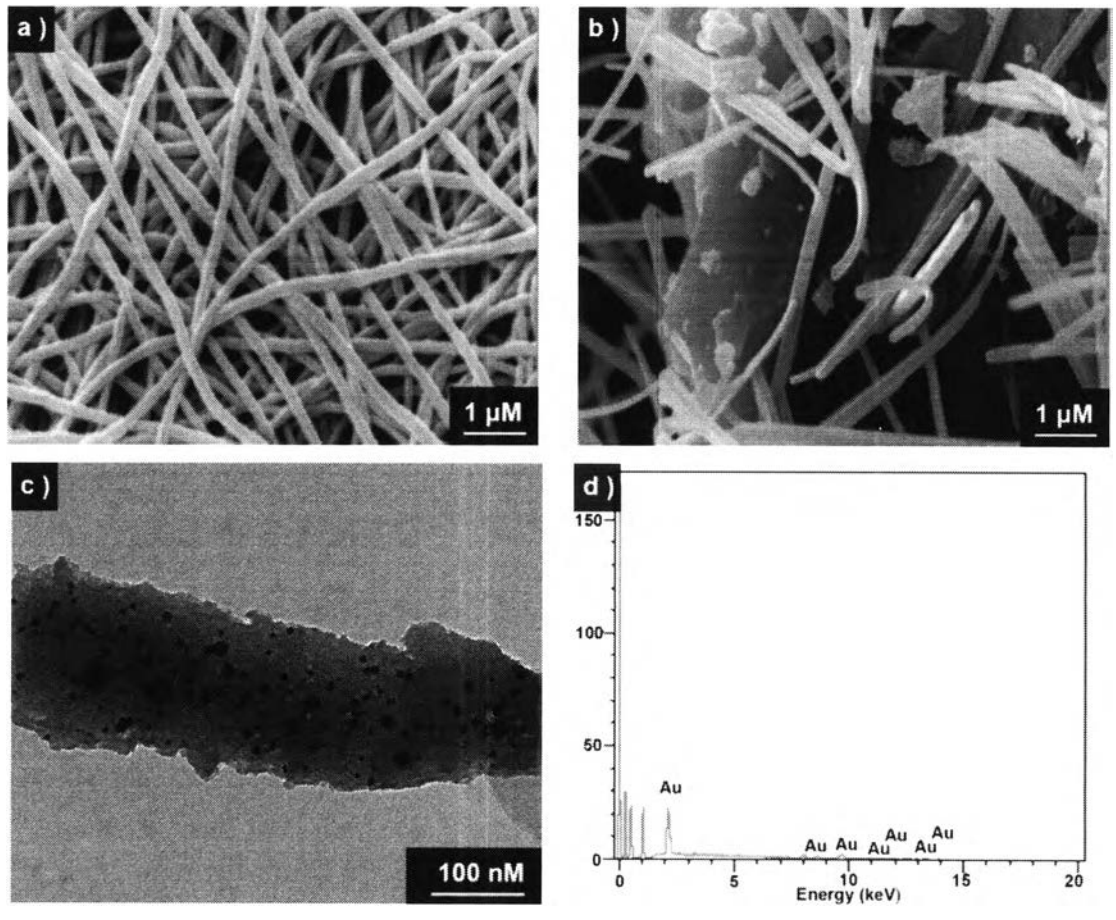

Figure 5.2 (a) SEM image of PAN-Au/G before carbonization, (b) SEM image of CPAN-Au/G after carbonization, (c) TEM image of CPAN-Au/G, and (d) EDX microanalysis spectrum of CPAN-Au/G.

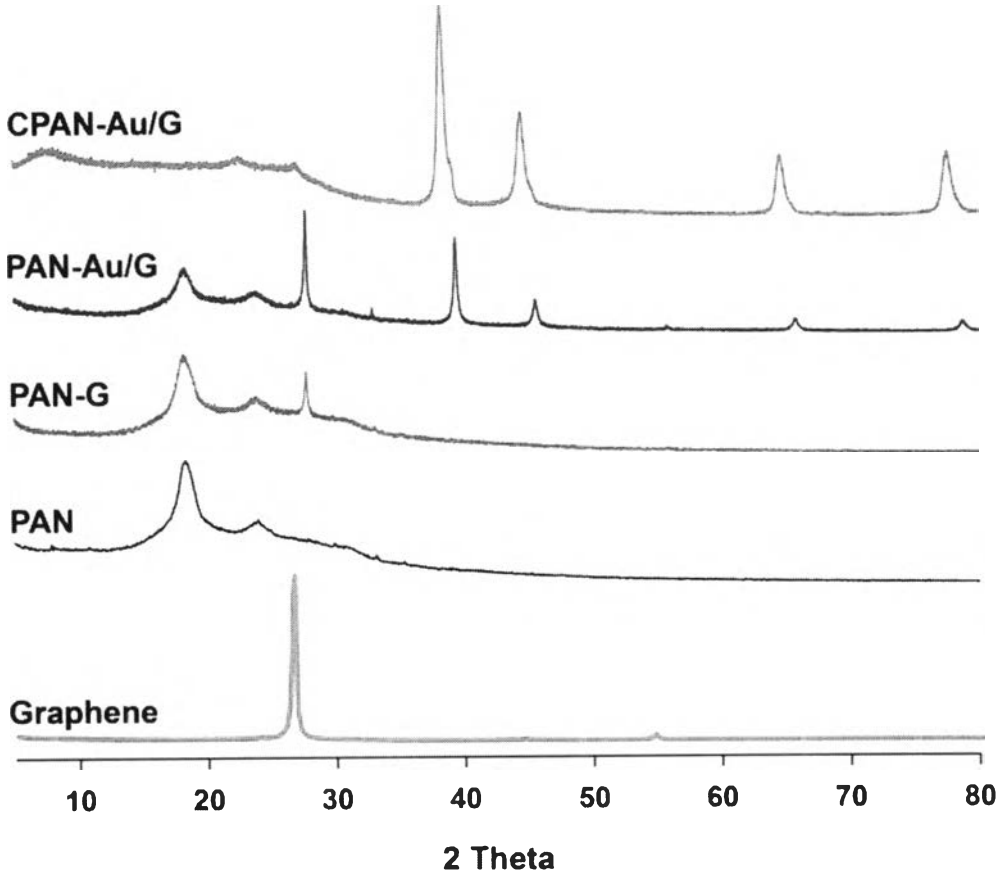

Figure 5.3 XRD patterns of graphene, PAN, PAN-G, PAN-Au/G, and CPAN-Au/G nanofibers.

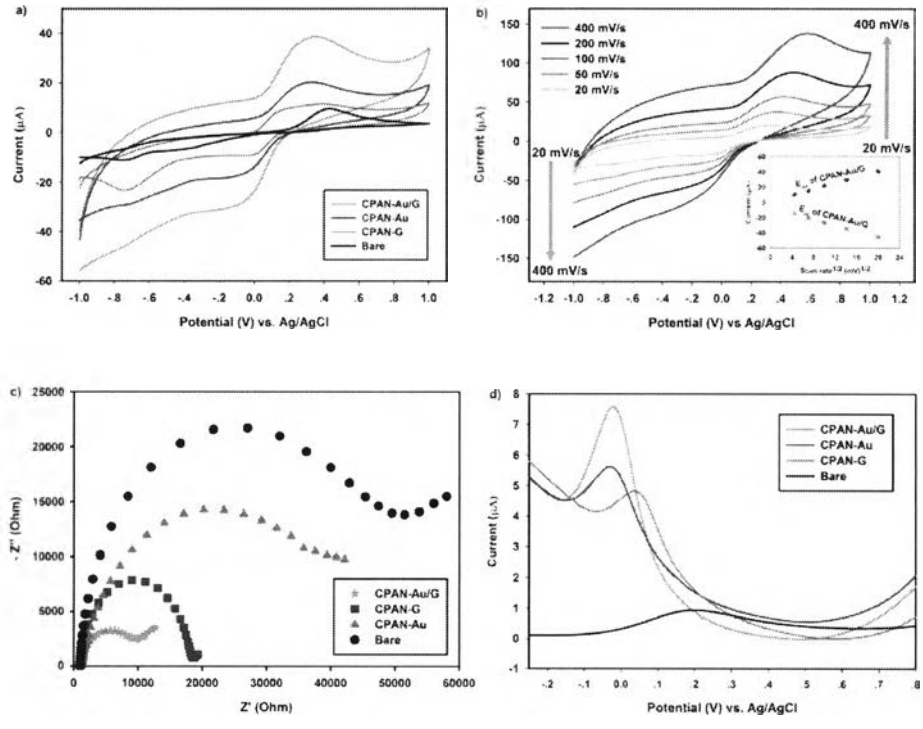

Figure 5.4 Electrochemical studies of unmodified/modified electrodes in 0.1 M PBS at pH 7.4; (a) CV at the various electrodes measured using 1 mM $[Fe(CN)_6]^{3-/4-}$, (b) CV at the CPAN-Au/G electrode measured using 1 mM $[Fe(CN)_6]^{3-/4-}$ at different scan rates, (c) EIS of various electrodes in 1 mM $[Fe(CN)_6]^{3-/4-}$ and (d) . DPV profiles of the unmodified and modified electrodes in the presence of 40 μM DA.

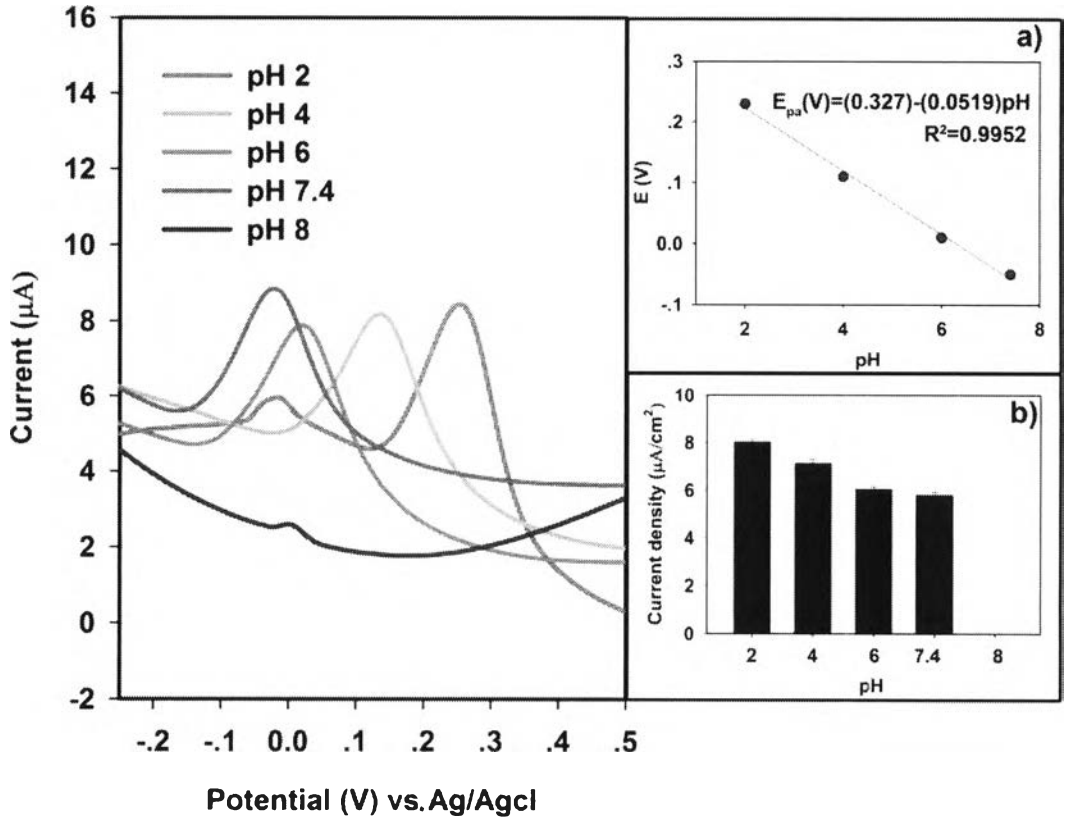

Figure 5.5 DPV of 40 μM DA in 0.1 M PBS at various pH levels at the CPAN-Au/G electrode. The insets are (a) current density of CPAN-Au/G at various pH levels and (b) the plots of oxidation potential at various pH levels.

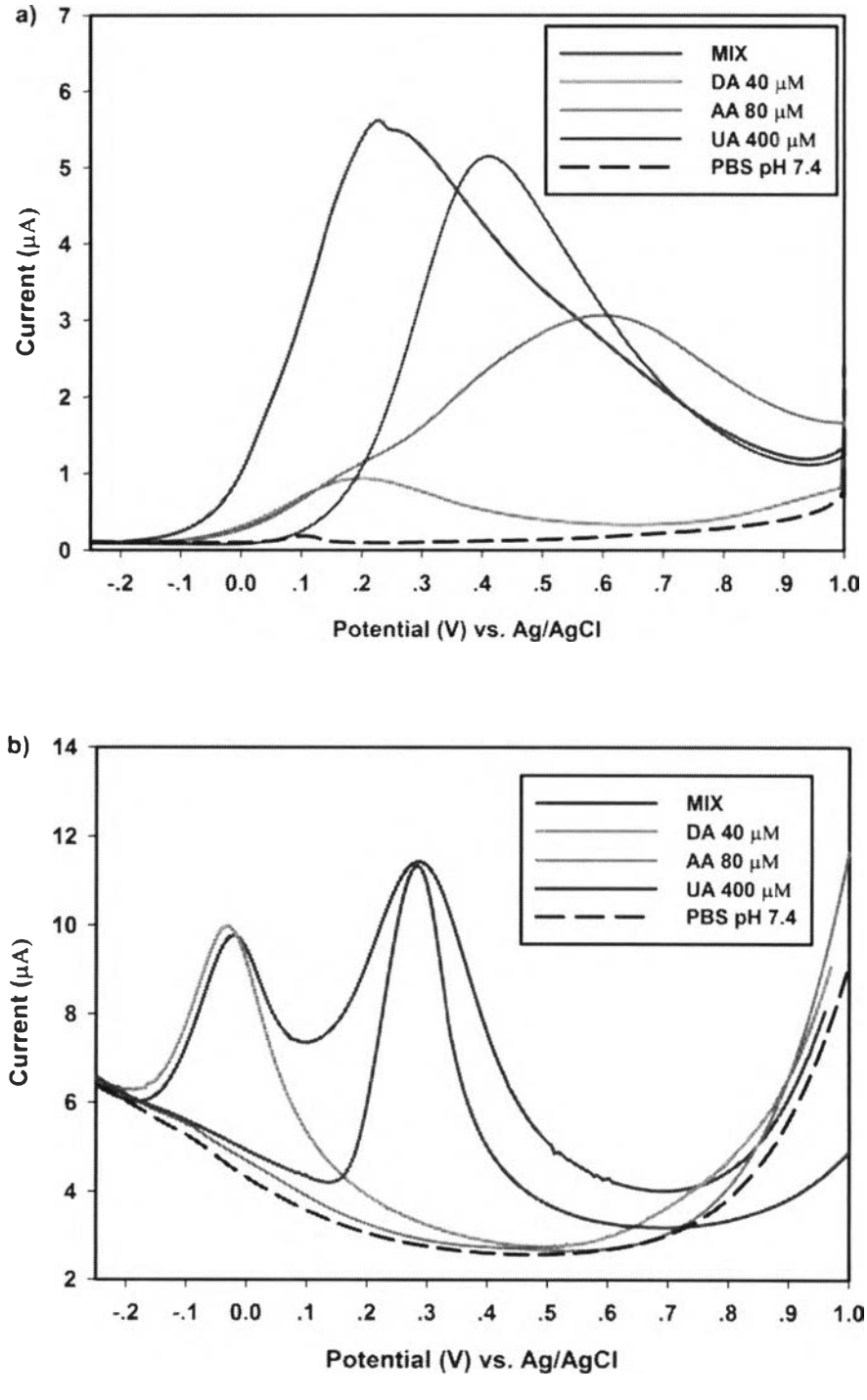

Figure 5.6 DPV of 40 μM DA, 80 μM AA, and 400 μM UA in 0.1 M PBS at pH 7.4 at electrodes; (a) bare SPCE and (b) CPAN-Au/G electrode.

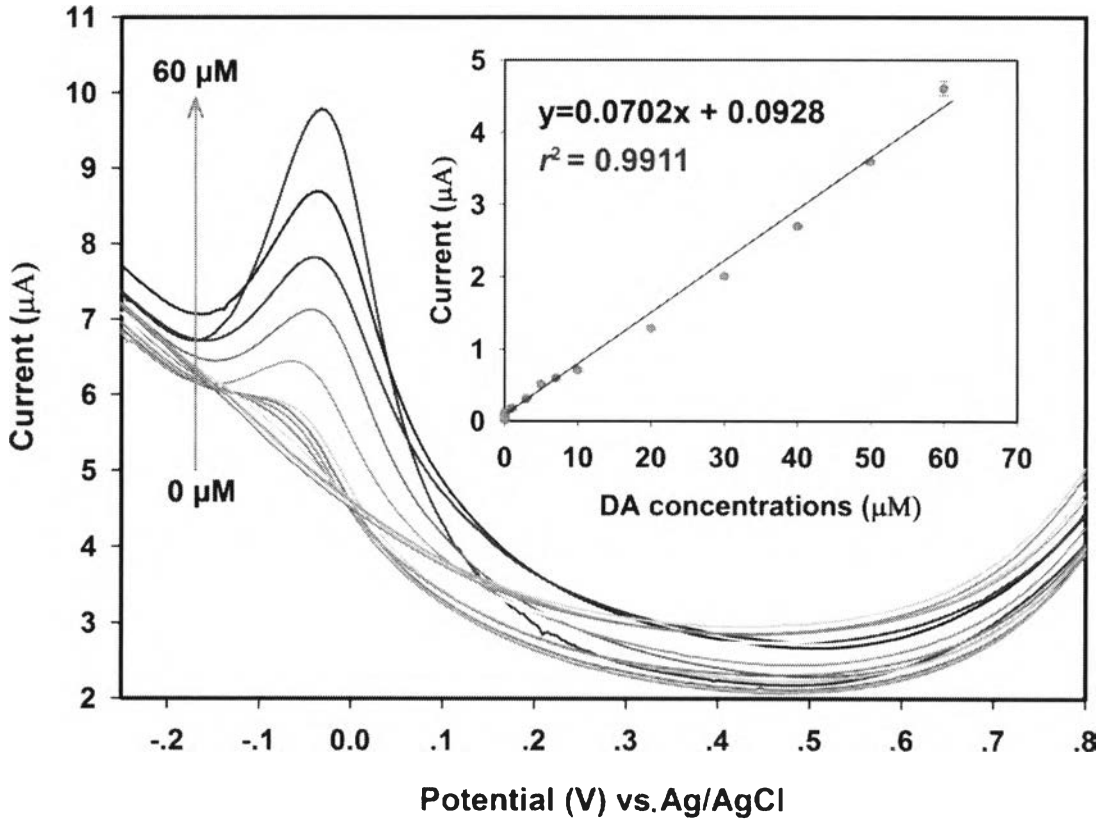

Figure 5.7 Representative DPV of 0.1 M PBS at pH 7.4 at the CPAN-Au/G electrode. The inset of the calibration curve for DA detection over a concentration range of 0-60 µM.

Table 5.1 Electrochemical data for each modified electrode

Electrode	Fiber diameter (nm)		Electrochemical parameters						
			1 mM $[Fe(CN)_6]^{3-/4-}$					40 μM DA[a]	
	Before CBZ	After CBZ	I_{pa}* (μA cm^{-2})	E_{pa}* (mV)	I_{pa}/I_{pc}*	ΔE_p* (mV)	R_p[b] (kΩ)	I_{pa} (μA cm^{-2})	E_{pa} (mV)
Bare SPCE	-	-	17.7 ±0.2	431	1.36	780	56 ±3	1.82 ±0.1	200
CPAN-G	151 ±21	144 ±19	20.5 ±0.7	170	1.08	142	43 ±1	2.87 ±0.2	30
CPAN-Au	187 ±20	128 ±31	21.7 ±0.8	272	1.04	346	18 ±3	3.73 ±0.1	-30
CPAN-Au/G	217 ±30	142 ±26	37.7 ±0.6	310	1.01	323	11 ±2	8.16 ±0.1	-30

* denotes CV with a scan rate of 50 mV s^{-1} in 0.1 M PBS at pH 7.4 (n=3).

a denotes DPV in 0.1 M PBS at pH 7.4 (n=3).

b denotes EIS in 0.1 M PBS at pH 7.4;

CBZ denotes the carbonization process.

Table 5.2 Comparison of the proposed electrode to other modified electrodes for DA detection.

Electrode	Method	pH	LDR (μM)	Sensitivity ($\mu A\ \mu M^{-1}$)	LOD (μM)	Reference
CDDA/GCE	DPV	7.0	5-205	0.106	0.61	(Ensafi *et al.*, 2009)
G/GCE	DPV	7.0	4-100	0.065	2.64	(Kim, 2010)
G-Au film/GCE	DPV	6.0	5-1000	-	1.86	(Li, 2012)
TiO_2-G/GCE	DPV	7.0	5-200	0.046	2	(Fan *et al.*, 2011)
GO/GCE	DPV	5.0	1.0-15	0.666	0.27	(Gao *et al.*, 2013)
BDD	DPV	7.0	5-100	0.075	1.1	(Guo-hua *et al.*, 2007)
Tiron/GCE	DPV	3.0	0.2-45.8	-	0.7	(Ali A. Ensaf, 2010)
Carbonized G/Au CNF/SPCE	DPV	7.4	0.001-60	0.0702	0.0008	This study

LDR is linear dynamic response; CDDA is poly 3-(5-chloro-2-hydroxyphenylazo)-4,5-dihydroxynaphthalene-2,7-disulfonic acid; GCE is glassy carbon electrode; G is graphene; Au is gold; BDD is boron-doped diamond electrode